

# Transparent glass-ceramics for optical applications

O. Dymshits, M. Shepilov, and A. Zhilin

The design, properties, and applications of transparent glass-ceramics are reviewed. Interference effects in light scattering by transparent glass-ceramics are discussed. The scattering coefficient of transparent glass-ceramics is found to be significantly less than that for the case of independent Rayleigh scattering by nanocrystals; its wavelength dependence is qualitatively different. A reduction in interference effects achieved by precipitation of nanocrystals of different crystalline phases with different scattering properties results in glass-ceramics with high diffuse reflection. The origin of the low coefficient of thermal expansion of glass-ceramics is discussed based on the temperature dependence of the unit cell parameters of β-quartz solid solutions measured by *in situ* high-temperature x-ray diffraction. Transparent glass-ceramics doped with $Co^{2+}$ and $Ni^{2+}$ ions for thermal shock-resistant color filters, for broadband near-infrared (IR) optical amplifiers, and for passive Q-switching of eye-safe Er lasers are presented. Glass-ceramics with rare-earth titanates, titanates-zirconates, and niobates in dual roles of nucleators and active crystals are reviewed.

## Introduction

Glass-ceramics for optical applications are easy and flexible to manufacture, and are more cost efficient than corresponding single crystals and optical ceramics. Higher optical quality, larger samples, and higher doping concentrations can be achieved in glass-ceramics. Some crystals precipitated in glass-ceramics are difficult or impossible to obtain in single crystal form. Moreover, a variety of metastable and stable crystals can be obtained in the same glass by appropriate heat treatments.

Glass-ceramics, in contrast to glasses, have optical properties similar to those of the single crystals, including well-defined structures with long-range order that is missing in glasses, specific properties determined by active ion position in the crystal structure leading to relatively narrow spectroscopic absorption and emission lines, and unique functionality inherent to noncentrosymmetric crystals (e.g., second-harmonic generation, piezoelectricity, electro-optic effects). One drawback of glass-ceramics is that active ions are not only located in the desired crystal phase, but may also be distributed between and at the interfaces of both crystalline and amorphous phases. Optical glass-ceramics are produced by melt-quenching, sinter-crystallization,[1] and laser patterning.[2,3] Glass-ceramic fibers have also been developed.[3–5] This article concentrates on materials that are not only promising optical glass-ceramics, but also within the field of our research for many years.

## Light scattering in glass-ceramics

Some demanding optical applications requirements can be met by transparent glass-ceramics. All glass-ceramics have inhomogeneous structure since they contain crystals distributed in glass. This inhomogeneity causes light scattering. In glass-ceramics for transparent optical elements, scattering needs to be reduced to a minimum. However, for diffuse reflection standards, light scattering is the determining property.

Previously, it was stated[6–8] that the scattering coefficient (turbidity) of glass-ceramics varies in a wide interval of wavelengths λ (e.g., in the range of visible light) according to the power law $\lambda^{-p}$, where $(-p)$ is the exponent of constant value, and $p \leq 4$. If the crystals are randomly distributed in the glass and are much smaller than the wavelength, then $p = 4$ (Rayleigh scattering).

Our studies[9,10] as well as analysis of published data[11,12] show that glass-ceramics frequently demonstrate "anomalous light scattering"[13] with $p > 4$ (up to 9). This effect is a result of interference of light scattered by different crystals demonstrating short-range ordering in their mutual arrangement.[14] Interference can reduce light scattering by several

O. Dymshits, NITIOM Vavilov State Optical Institute, Russia; vodym1959@gmail.com
M. Shepilov, NITIOM Vavilov State Optical Institute, Russia; m.shep@mail.ru
A. Zhilin, NITIOM Vavilov State Optical Institute, Russia; zhilin1311@mail.ru
doi:10.1557/mrs.2017.29


© 2017 Materials Research Society
https://doi.org/10.1557/mrs.2017.29 Published online by Cambridge University Press

times or more.[13,14] This is demonstrated for $Na_2O$-$Nb_2O_5$-$SiO_2$ glass crystallization by the optical studies data (**Figure 1**) supplemented by x-ray diffraction data for $NaNbO_3$ nanocrystals.[9] At the early stage of heat treatment (time $t$ = 2, 4, and 6 h), scattering is close to Rayleigh scattering ($p \cong 4.5$–$4.8$, see inset in Figure 1). At this stage, turbidity increases with the number of $NaNbO_3$ nanocrystals per unit volume according to x-ray diffraction data. As the number of nanocrystals further increases during longer heat treatments ($t > 6$ h), when their volume fraction becomes greater than ≈0.2 and increases up to ≈0.3, interference suppresses scattering, yielding $p \cong 6.2$ and reducing turbidity.

The greater the dispersion of scattering properties of crystals in glass-ceramics, the lower the interference and greater the scattering.[15] Based on this approach, glass-ceramics for laser components and standards of whiteness with high diffuse reflectance have been developed.[16]

## Systems for transparent glass-ceramics

Transparent glass-ceramics have been fabricated from many systems thus far and depending on the system, can be used for various applications. For example, glass-ceramics can be based upon "stuffed" β-quartz solid-solution structures with network replacement of $Si^{4+}$ by $Al^{3+}$ accompanied by filling of interstitial vacancies by $Li^+$, $Mg^{2+}$, and $Zn^{2+}$ cations to preserve electrical neutrality[17]—in the $Li_2O$-MgO-ZnO-$Al_2O_3$-$SiO_2$ system with titania and/or zirconia as nucleators;[6,7,17,18] spinels in the (Li, Na, K, Mg, Zn)O-(Al, Ga)$_2O_3$-(Si, Ge)$O_2$ system[3,6,7,17,19,20] with or without nucleators; mullite in the $Al_2O_3$-$SiO_2$ system[6,17] with BaO, $K_2O$, or $Cs_2O$ additions; forsterite in the $K_2O$-MgO-$Al_2O_3$-$SiO_2$ system nucleated by $TiO_2$;[17] on ZnO or β-willemite in the $K_2O$-ZnO-$Al_2O_3$-$SiO_2$ system;[21] and mixed orthosilicates, $Mg_2SiO_4$-$Zn_2SiO_4$-$Li_4SiO_4$, in the $K_2O$-$Li_2O$-MgO-ZnO-$Al_2O_3$-$SiO_2$ system.[17] The distinct feature of these transparent glass-ceramics is that transition-metal (TM) ions ($Cr^{3+}$, $Cr^{4+}$, $Ni^{2+}$, $Co^{2+}$, $V^{4+}$, $Mn^{2+}$) can enter their crystalline phases, thus producing materials that can be used in broadband optical amplification, in tunable and IR lasers, in solar collectors, and as phosphors for solid-state lighting.

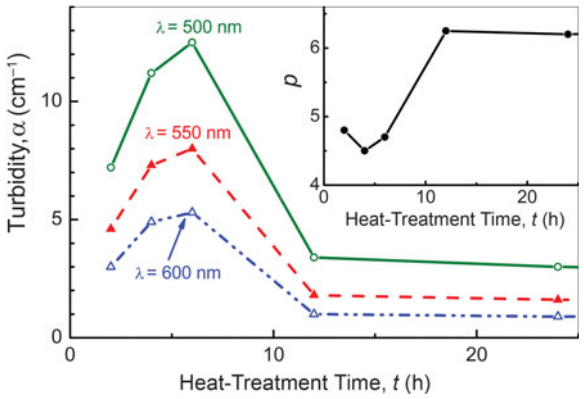



**Figure 1.** Turbidity α at three wavelengths λ (500, 550, and 600 nm) in the course of the crystallization of $Na_2O$-$Nb_2O_5$-$SiO_2$ glass as a function of heat-treatment time, $t$. At the early stage of crystallization ($t \leq 6$ h, volume fraction of $NaNbO_3$ nanocrystals is less than 0.2), turbidity increases with increasing number of independent scatterers (nanocrystals) per unit volume. As the number of nanocrystals further increases (at $t > 6$ h, volume fraction becomes greater than 0.2 and increases up to ≈0.3), interference leads to a decrease in turbidity. At a given heat-treatment time, $t$, the wavelength dependence of the turbidity is described by the power law $\lambda^{-p}$ and characterized by the magnitude of $p$. The inset shows values of $p$ for different heat-treatment times. At the early stage ($t \leq 6$ h), $p \cong 4.5$–$4.8$, close to the Rayleigh value of 4 that is characteristic of small independent scatterers (nanocrystals). At $t > 6$, interference leads to $p \cong 6.2$ (anomalous scattering).[9]

The (Li, Na, K, Mg, Zn)O-(Al, Ga)$_2O_3$-(Si, Ge)$O_2$ system[3,6,7,17,19,20] with or without nucleators; mullite in the $Al_2O_3$-$SiO_2$ system[6,17] with BaO, $K_2O$, or $Cs_2O$ additions; forsterite in the $K_2O$-MgO-$Al_2O_3$-$SiO_2$ system nucleated by $TiO_2$;[17] on ZnO or β-willemite in the $K_2O$-ZnO-$Al_2O_3$-$SiO_2$ system;[21] and mixed orthosilicates, $Mg_2SiO_4$-$Zn_2SiO_4$-$Li_4SiO_4$, in the $K_2O$-$Li_2O$-MgO-ZnO-$Al_2O_3$-$SiO_2$ system.[17] The distinct feature of these transparent glass-ceramics is that transition-metal (TM) ions ($Cr^{3+}$, $Cr^{4+}$, $Ni^{2+}$, $Co^{2+}$, $V^{4+}$, $Mn^{2+}$) can enter their crystalline phases, thus producing materials that can be used in broadband optical amplification, in tunable and IR lasers, in solar collectors, and as phosphors for solid-state lighting.

There are glass-ceramics based on fluoride crystals in oxyfluoride systems,[22–25] upon fresnoite-type crystals in the BaO-$TiO_2$-(Si,Ge)$O_2$ system,[2,26] upon various niobium-containing phases in the (Li, Na, K)$_2O$-$Nb_2O_5$-(Ge, Si, Te)$O_2$[2,9,26–28] system, upon yttrium aluminum garnet in the $Y_2O_3$-$Al_2O_3$-$SiO_2$-$Li_2O$-$TiO_2$-$ZrO_2$ system,[29] upon halogenides in the fluorozirconate[30] system, and upon chalcogenides.[31] In these transparent glass-ceramics, rare-earth (RE) ions enter the crystalline phase, allowing for their use in solid-state lasers, fiber amplifiers, solid-state lighting, and color displays. There are several excellent reviews[2,3,8,23–26,28,29,31–35] devoted mainly to these transparent glass-ceramics that will not be discussed here.

## Low-expansion glass-ceramics

Glass-ceramics based upon lithium aluminosilicate crystals with the β-quartz solid-solution structure in the $Li_2O$-$Al_2O_3$-$SiO_2$ (LAS) system that combine high transparency, near-zero coefficient of thermal expansion (CTE), excellent optical polishability, and strength[6,17,18] are used in the most important precision optical applications for telescope mirrors, laser gyroscopes, and optical parts. In addition, low-CTE, near-IR transparent LAS glass-ceramics form the foundation for glass-ceramic cooktop panels. In all of these transparent glass-ceramics, the substitution of ($SiO_4$) units in the β-quartz structure by ($AlO_4$) ones is achieved with charge compensation by $Li^+$, $Mg^{2+}$, $Zn^{2+}$, or by $AlPO_4$.[17,18]

It was demonstrated by *in situ* high-temperature x-ray diffraction analysis[36] that in glass-ceramics with $SiO_2$ content ranging from 44–70 mol%, the CTE of disordered β-quartz solid-solution nanocrystals is near zero or slightly negative. The residual glass is highly siliceous with small $TiO_2$ and $Al_2O_3$ content, and its CTE is close to zero. The CTE of transparent glass-ceramics with high crystallinity fraction is thus determined to a large extent by the CTE value of the crystalline phase.[6,36] The precise tailoring of the glass composition and crystallization schedule allows for adjustment of CTE values to zero.[18]

### *Thermal shock-resistant color filters*

Attracted by excellent transparency and low CTE values of glass-ceramics in the LAS system, we have developed violet, blue, green, red, purple, and neutral thermal shock-resistant color filters for laser systems and high-power light sources



https://doi.org/10.1557/mrs.2017.29 Published online by Cambridge University Press

that can operate in high-temperature gradient fields, for instance, as aircraft signal lamps.[37] Spinel nanocrystals precipitate in these materials in a narrow "low-temperature" range of 720–770°C. TM ions enter their structure, while prolonged heat treatments lead to crystallization of β-quartz solid solution without decomposition of spinel crystals, resulting in transparent glass-ceramics with low CTE and unusual coloration. At elevated temperatures of 780–900°C that prevent spinel crystallization, TM ions entering the β-quartz solid solution produced differently colored thermal shock-resistant transparent glass-ceramics. Different tints can be obtained in the transparent glass-ceramics with the same composition by varying the heat-treatment temperature (e.g., $Ni^{2+}$ ions in spinel nanocrystals produce green, and in β-quartz solid solution, the ions produce purple and red coloration[38] [**Figure 2**]).

## Transparent glass-ceramics for broadband amplifiers and tunable lasers

The limited bandwidth of RE ion-doped amplifiers caused by narrow luminescent bandwidths of their 4*f*–4*f* optical transitions is a problem of communication technology. TM ions such as $Ni^{2+}$ in octahedral coordination exhibit broadband near-IR emission with high quantum efficiency in crystals, yet there is no luminescence in Ni-doped glasses. Therefore, development of glass-ceramics suitable for fiber drawing with crystalline phases containing $Ni^{2+}$ ions in octahedral position could solve this problem. Pinckney and Beall[17] demonstrated that transparent glass-ceramics based upon various spinels show wide-IR luminescence when doped with $Ni^{2+}$ ions located in octahedral positions.

Further investigations by many research groups developed novel transparent glass-ceramics based on spinels and other crystals wherein $Ni^{2+}$ ions located in octahedral sites and evaluated their spectral properties. Studies[3,39] showed that one can control the strength of the local ligand field and the local symmetry around $^{[VI]}Ni^{2+}$ ions by precise tailoring of the transparent glass-ceramic composition, the nature and content of nucleating agents, the NiO concentration, and heat-treatment conditions. Some transparent glass-ceramics were developed containing a single crystalline phase with different octahedral sites. Other transparent glass-ceramics contain a combination of different crystalline phases where $Ni^{2+}$ ions act as a single emission species in multiple octahedral local environments,[3] which leads to broadening of the IR luminescent band. Energy transfer from $Cr^{3+}$ ions to $Ni^{2+}$ in spinel and from $Yb^{3+}$ ions in glass to $Ni^{2+}$ ions in spinel was achieved, increasing the luminescence intensity, while additions of $Er^{3+}$and Bi ions resulted in a broad-IR luminescence provided by independent active ions without energy transfer.[3] Broadband optical amplification in β-$Ga_2O_3$:$Ni^{2+}$-based transparent glass-ceramics was demonstrated.[3]

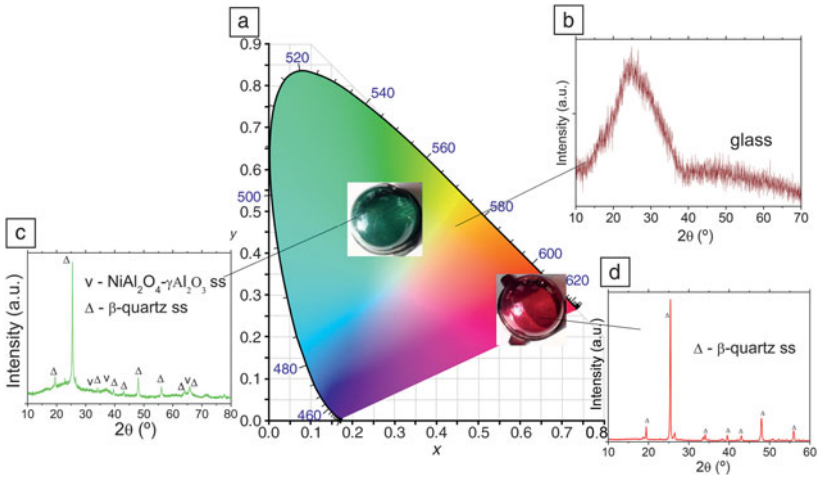



**Figure 2.** (a) Images of green and red aircraft navigation lights made of Ni-doped $Li_2O$-$Al_2O_3$-$SiO_2$ transparent glass-ceramic; color coordinates in the Commission Internationale de l'Eclairage (CIE) chromaticity diagram, an international standard for primary colors that allows all other colors to be defined as a weighted sum of the three primary colors, and x-ray diffraction patterns of (b) the initial glass and transparent glass-ceramic, which is (c) green due to $Ni^{2+}$ absorption in spinel nanocrystals and (d) red due to $Ni^{2+}$ absorption in nanocrystals of β-quartz solid solution.[37,38] The blue numbers on the main plot represent wavelengths. When the initial brown-colored amorphous glass, whose x-ray pattern is presented in (b) and whose color coordinates are shown, is heat-treated at 720–770°C, (c) it transforms into a thermal shock-resistant green-colored glass-ceramic containing nanocrystals of $Ni^{2+}$-doped spinel and β-quartz solid solution. (b) The position of the green signal lamp image on the CIE chromaticity diagram shows the color coordinates of green glass-ceramics. (d) When prepared by heat treatments at elevated temperatures of 780–900°C, red-colored transparent glass-ceramics contain nanocrystals of $Ni^{2+}$-doped β-quartz solid solution. (b) The position of the red signal lamp image on the CIE chromaticity diagram shows the color coordinates of red glass-ceramics. Note: ss, solid solution; *x*, *y*, chromaticity coordinates; 2θ, diffraction angle.

## Transparent glass-ceramics for passive Q-switching of Er-lasers

"Eye-safe" Er lasers with emission wavelengths approximately 1.5–1.7 μm are used for applications that involve human contact with laser radiation and require short (nanosecond long) high peak power pulses that can be produced via passive Q-switching, a method for obtaining such pulses by modulating the intracavity losses by a saturable absorber (SA) inserted into the laser cavity. In SAs, absorption decreases with increasing fluence of the incident radiation. Materials for SAs need to have an absorption band that matches the laser emission wavelength, provide low saturation fluence and low nonsaturable losses, fast recovery time of the initial absorption, and high laser damage threshold. SAs based on $Co^{2+}$:$MgAl_2O_4$ spinel single crystals were acknowledged as the best for Er, Yb:glass lasers with an emission wavelength of ~1.54 μm. In these crystals, $Co^{2+}$ ions with $3d^7$ electronic configuration are predominantly located in tetrahedral sites, and their broadband IR absorption perfectly matches the ~1.54 μm Er emission wavelength. Boiko et al.[40] were the


https://doi.org/10.1557/mrs.2017.29 Published online by Cambridge University Press

first to introduce $Co^{2+}$-doped transparent glass-ceramics based on spinel-type gahnite ($ZnAl_2O_4$) crystals as SAs. Following this, transparent glass-ceramics based on $Co^{2+}$-doped spinel $MgAl_2O_4$ nano-sized crystals were introduced.[41,42] A comparison with $Co^{2+}$:$MgAl_2O_4$ single crystals demonstrated that glass-ceramics based on Co-doped $MgAl_2O_4$ spinel nanocrystals are good competitors to corresponding single crystals.[42] Based on these encouraging results, transparent glass-ceramics for SAs with $^{IV}Co^{2+}$-doped nano-sized crystals of different spinels[37,40,41] were developed in ZnO-$Al_2O_3$-$SiO_2$ (ZAS), MgO-$Al_2O_3$-$SiO_2$ (MAS), and LAS systems. Other transparent glass-ceramics for SAs were also suggested.[43]

Motivated by the recent progress in directly pumped Er crystal lasers that provide oscillations at 1.6–1.7 μm, a new series of SAs based on transparent glass-ceramics were developed whose distinct feature is a shift of the absorption band of $^{IV}Co^{2+}$ ions to longer wavelengths due to the lower ligand field strength around $Co^{2+}$ ions as compared to that in $MgAl_2O_4$ spinel (**Table I**).[44]

Glass-ceramics with RE ions embedded into crystalline phases have been studied in the search for efficient photoluminescent and up-conversion materials. An attractive idea to introduce RE ions into LAS glass-ceramics was not realized because β-quartz solid solution is a poor host for fluorescent cations.[17,25] Recently, researchers were able to incorporate RE ions into the crystalline phases of aluminosilicate glass-ceramics, where these crystalline phases were not β-quartz solid solution, but RE titanates, titanites-zirconites, and niobates.[38,45–49] Similar to RE fluorides, these nanocrystals ensure a low-phonon energy lattice surrounding the RE ions, but these glass-ceramics possess high thermomechanical properties and their compositions are highly reproducible.

## Transparent glass-ceramics based on nano-sized crystals of RE titanates and titanates-zirconates

When LAS or MAS glasses nucleated by $TiO_2$ or $ZrO_2$ are doped with RE ions, $RE_2(Ti, Zr)_2O_7$ crystals with the defect-fluorite structure precipitate.[38,45–47] At elevated temperatures, a disordered and then ordered pyrochlore-type structure is formed.

When doped with $Er^{3+}$ and $Yb^{3+}$ ions, these transparent glass-ceramics demonstrate substantial enhancement (near 10×) of red up-conversion emission around ~650 nm,[47] which is important for phosphors and solid-state lightning. They are also candidates for a medium for effective laser generation in the spectral range of 1.5 μm.[38]

**Table I. Saturation intensity $F_S$ (at ~1.54 μm), recovery time τ, and long-wavelength edge of the infrared ($^4A_2(^4F)\rightarrow{}^4T_1(^4F)$) absorption band of $^{IV}Co^{2+}$ ions, $\lambda_{th}$, for several $Co^{2+}$-doped materials.[44]**

| Material | $F_S$, J/cm² | τ, ns | $\lambda_{th}$, μm |
|---|---|---|---|
| Single crystals | | | |
| $MgAl_2O_4$ | 0.4–0.5 | 220–420 | 1.58 |
| Crystalline phase in TGC | | | |
| $MgAl_2O_4$ | 0.4 | 280 | 1.63 |
| $ZnAl_2O_4$ | 0.6–0.7 | 650–900 | 1.56 |
| $Mg(Al,Ga)_2O_4$ | 0.45–0.7 | 240–335 | 1.67 |
| ZnO | 0.8 | 895 | 1.73 |
| ZnO + β-$Zn_2SiO_4$ | 0.75 | 820 | 1.74 |
| γ-$Ga_2O_3$ | 0.8 | 166 | 1.78 |

Note: TGC, transparent glass-ceramic.

## Transparent glass-ceramics based on nano-sized crystals of RE orthoniobates

Recently, transparent glass-ceramics with the RE niobate nanophase in the dual role of luminescent active crystal and nucleator of β-quartz solid solution in LAS glasses were prepared.[48,49] The optical properties of these glass-ceramics were directly linked to the structure of RE niobates, which changes from the defect fluorite to the tetragonal, and then, to the monoclinic form (**Figure 3**). $RENbO_4$ nanocrystals provide promising spectral-luminescent properties while the large amount of β-quartz solid solution ensures high thermal shock resistance of the glass-ceramics. Transparent glass-ceramics with the tetragonal (Er, Yb)$NbO_4$ nanophase have potential for laser operation in the eye-safe region.[48] $RENbO_4$-based transparent glass-ceramics are interesting materials for double ($RE^{3+}$, $Yb^{3+}$) or triple ($RE_1^{3+}$, $RE^{23+}$, $Yb^{3+}$) codoping for color-tunable phosphors in the visible region, for generation of warm/cold white light.[49]

## Summary

Detailed knowledge of the sequence of phase transformations in the course of glass-ceramic formation is required to find the balance between (a) maximizing the fraction of desired crystalline phase accommodating active ions; (b) minimizing the fractions of crystalline and amorphous phases accommodating active ions in coordinations different from that desired; and (c) minimizing scattering losses.

Based on this strategy, transparent glass-ceramics doped with $Co^{2+}$ and $Ni^{2+}$ ions for thermal shock-resistant color filters, for broadband near-IR optical amplifiers, and for passive Q-switching of eye-safe Er lasers as well as glass-ceramics with RE titanates, titanates-zirconates, and niobates in dual roles of nucleators and active crystals were developed. The selective partition of transition-metal ions into the crystals with spinel structure and of RE ions into titanate, titanate-zirconate, niobate, and fluoride crystals is an approach to the design of new multifunctional materials. In addition to traditional melt quenching and sinter crystallization, laser patterning and glass-ceramic melt-in-tube fiber drawing are fascinating methods for forming glass-ceramics that broaden the compositions and shaping of transparent glass-ceramics.

## Acknowledgments

The authors express their gratitude to the Russian Foundation for Basic Research (Grant 16-03-01130) for partial support of this work. We also thank M.J. Davis for his valuable suggestions and comments.



https://doi.org/10.1557/mrs.2017.29 Published online by Cambridge University Press

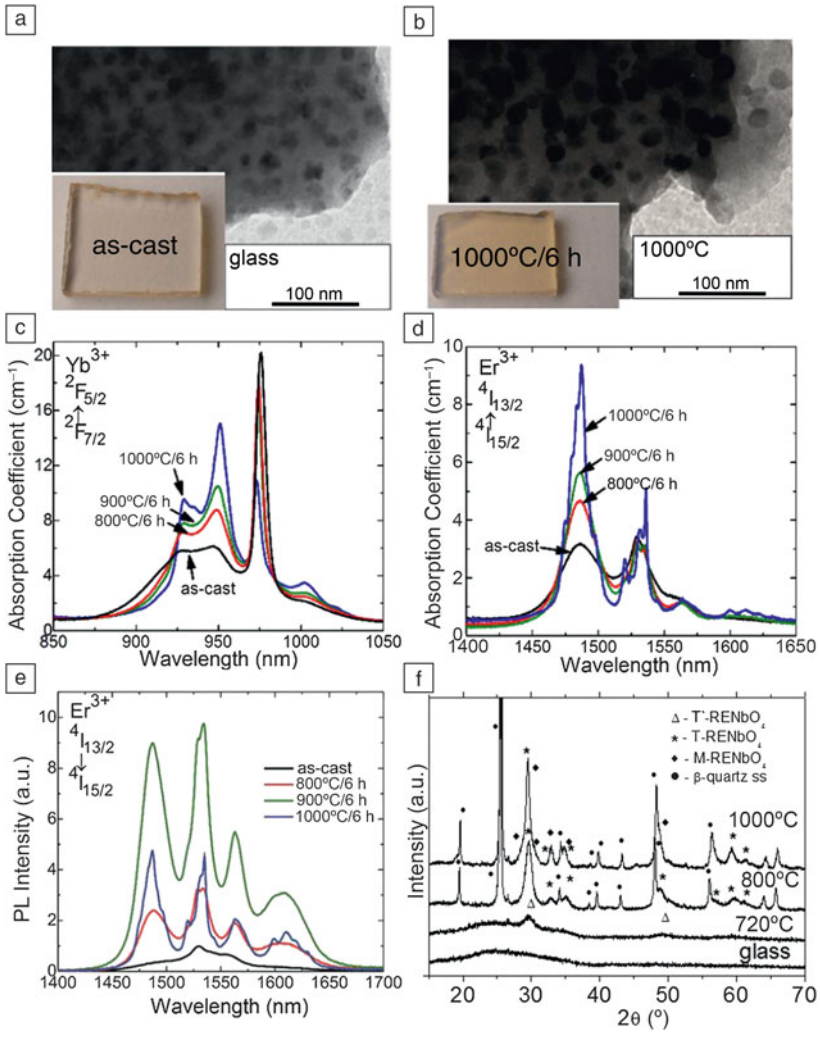



**Figure 3.** (a) Image of polished sample (inset) and transmission electron microscope (TEM) image of lithium aluminosilicate glass doped with $Er_2O_3$, $Yb_2O_3$, and $Nb_2O_5$; (b) Image of polished sample (inset) and TEM image of lithium aluminosilicate glass-ceramics doped with $Er_2O_3$, $Yb_2O_3$, and $Nb_2O_5$ prepared at 1000°C for 6 h.[48] The value indicated in the figure denotes heat-treatment schedule. Both TEM images demonstrate nearly uniform distribution of inhomogeneous regions (dark regions) without any clustering. The sizes of the regions of inhomogeneity are approximately 10 nm in the initial glass and approximately 15 nm after the heat treatment. (c) Absorption spectra related to the $^2F_{7/2} \rightarrow {}^2F_{5/2}$ ($Yb^{3+}$) transition for the initial glass and glass-ceramics containing (Er, Yb)$NbO_4$ nanocrystals. (d) Absorption spectra related to the $^4I_{15/2} \rightarrow {}^4I_{13/2}$ ($Er^{3+}$) transition for the initial glass and glass-ceramics containing (Er, Yb)$NbO_4$ nanocrystals after the indicated heat-treatment schedules. (e) Near-infrared photoluminescence of $Er^{3+}$ ions for the initial glass and glass-ceramics doped with $Er_2O_3$, $Yb_2O_3$, and $Nb_2O_5$ and prepared at 800, 900, and 1000°C for 6 h; the excitation wavelength is 960 nm. (f) X-ray diffraction patterns of the initial and heat-treated glasses doped with 3 mol% $Yb_2O_3$ and 3 mol% $Nb_2O_5$ at the indicated heat-treatment temperatures and duration. Patterns are shifted for ease of observation. The absorption and luminescent properties of these glass-ceramics are directly linked to the structure of rare-earth (RE) niobates, which change structure from the defect fluorite to tetragonal and then to monoclinic due to heat treatment. RE orthoniobates provide promising spectral-luminescent properties, while the crystallization of a large amount of β-quartz solid solution ensures near-zero coefficient of thermal expansion of these novel, transparent glass-ceramics. Note: 2θ, diffraction angle; PL, photoluminescence; T′, crystals with disordered fluorite-type structure; T, crystals with tetragonal structure; M, crystals with monoclinic structure; ss, solid solution.[48,49]

## References


1. M.O. Prado, E.D. Zanotto, *C. R. Chim.* **5**, 773 (2002).
2. T. Komatsu, *J. Non Cryst. Solids* **428**, 156 (2015).
3. J. Qiu, *Int. J. Appl. Glass Sci.* **7**, 270 (2016).
4. K.E. Downey, B.N. Samson, G.H. Beall, E.J. Mozdy, L.R. Pinckney, N.F. Borrelli, A. Mayolet, *Conf. Lasers Electro-Opt.* **56**, 211 (2001).
5. V.M. Mashinsky, N.M. Karatun, V.A. Bogatyrev, V.N. Sigaev, N.V. Golubev, E.S. Ignat'eva, R. Lorenzi, A. Paleari, E.M. Dianov, *Microsc. Microanal.* **18**, 259 (2012).
6. G.H. Beall, D.A. Duke, *J. Mater. Sci.* **4**, 340 (1969).
7. G.H. Beall, L.R. Pinckney, *J. Am. Ceram. Soc.* **82**, 5 (1999).
8. T. Berthier, V.M. Fokin, E.D. Zanotto, *J. Non Cryst. Solids* **354**, 1721 (2008).
9. M.P. Shepilov, O.S. Dymshits, V.V. Golubkov, A.A. Zhilin, *Adv. Mater. Res.* **39–40**, 273 (2008).
10. I.P. Alekseeva, O.S. Dymshits, A.A. Zhilin, S.S. Zapalova, M.P. Shepilov, V.V. Golubkov, A.E. Kalmykov, A.V. Myacoedov, *J. Opt. Technol.* **81**, 729 (2014).
11. S. Zhu, H. Ma, L. Calvez, X. Zhang, J. Lucas, J.-L. Adam, H. Shang, T. Rouxel, *J. Non Cryst. Solids* **353**, 1298 (2007).
12. M. Chavoutier, D. Caurant, O. Majérus, R. Boulesteix, P. Loiseau, C. Jousseaume, *J. Non Cryst. Solids* **384**, 15 (2014).
13. N.S. Andreev, *J. Non Cryst. Solids* **30**, 99 (1978).
14. M.P. Shepilov, *Phys. Chem. Glasses* **46**, 173 (2005).
15. M.P. Shepilov, *Opt. Mater.* **31**, 385 (2008).
16. A.V. Bortkevich, M.L. Varshavchik, O.S. Dymshits, A.A. Zhilin, S.M. Leykin, A.Y. Polushkin, M.M. Seredenko, T.I. Chuvaeva, A.V. Shashkin, *J. Opt. Technol.* **64** (8), 111 (1997).
17. W. Höland, G.H. Beall, Eds., *Glass-Ceramic Technology*, 2nd ed. (The American Ceramic Society/Wiley, New York, 2012).
18. H. Bach, D. Krause, Eds., *Low Thermal Expansion Glass Ceramics*, 2nd ed. (Springer-Verlag Berlin Heidelberg, 2005).
19. S. Chenu, E. Véron, C. Genevois, G. Matzen, T. Cardinal, A. Etienne, D. Massiot, M. Allix, *Adv. Opt. Mater.* **2**, 364 (2014).
20. Y. Zhuang, J. Ueda, S. Tanabe, *Appl. Phys. Lett.* **105**, 191904 (2014).
21. L.R. Pinckney, *Phys. Chem. Glasses Eur. J. Glass Sci. Technol. B* **47**, 127 (2006).
22. Y. Wang, J. Ohwaki, *Appl. Phys. Lett.* **63**, 3268 (1993).
23. A. de Pablos-Martín, A. Duran, M.J. Pascual, *Int. Mater. Rev.* **57**, 165 (2012).
24. P.P. Fedorov, A.A. Luginina, A.I. Popov, *J. Fluor. Chem.* **172**, 22 (2015).
25. J. Qiu, Q. Jiao, D. Zhou, Z. Yang, *J. Rare Earths* **34**, 341 (2016).
26. T. Komatsu, T. Honma, *Int. J. Appl. Glass Sci.* **4**, 125 (2013).
27. N.F. Borrelli, *J. Appl. Phys.* **38**, 4243 (1967).
28. H. Jain, *Ferroelectrics* **306**, 111 (2004).
29. S. Fujita, S. Tanabe, *Int. J. Appl. Glass Sci.* **6**, 356 (2015).
30. A. Edgar, J.M. Spaeth, S. Schweizer, S. Assmann, P.J. Newman, D.R. MacFarlane, *Appl. Phys. Lett.* **75**, 2386 (1999).
31. L. Calvez, "Transparent Chalcogenide Glass-Ceramics," in *Chalcogenide Glasses, Preparation, Properties and Applications*, J.-L. Adam, X. Zhang, Eds. (Woodhead Publishing, Oxford, UK, 2014).
32. M. Ferrari, G.C. Righini, *Int. J. Appl. Glass Sci.* **6**, 240 (2015).
33. G.H. Beall, *Int. J. Appl. Glass Sci.* **5**, 93 (2014).
34. E.D. Zanotto, *Am. Ceram. Soc. Bull.* **89**, 19 (2010).
35. C. Rüssel, C. Bocker, M. Stoica, K. Thieme, A. Keshavarzi, *J. Chem. Technol. Metall.* **50**, 357 (2015).
36. E. Artukh, V. Astakhova, A. Zhilin, C. Filatov, T. Chuvaeva, *Inorg. Mater.* (USSR) **2**, 408 (1992).
37. I. Alekseeva, O. Dymshits, M. Tsenter, A. Zhilin, V. Golubkov, I. Denisov, N. Skoptsov, A. Malyarevich, K. Yumashev, *J. Non Cryst. Solids* **356**, 3042 (2010).
38. O.S. Dymshits, A.A. Zhilin, T.I. Chuvaeva, M.P. Shepilov, *J. Non Cryst. Solids* **127**, 44 (1991).
39. P.A. Loiko, O.S. Dymshits, A.A. Zhilin, I.P. Alekseeva, K.V. Yumashev, *J. Non Cryst. Solids* **376**, 99 (2013).
40. R.M. Boiko, A.G. Okhrimchuk, A.V. Shestakov, in *Advanced Solid State Lasers*, OSA Trends in Optics and Photonics Series, vol. 19, W.R. Bosenberg, M.M. Fejer, Eds. (Optical Society of America, Washington, DC, 1998), p. 185.

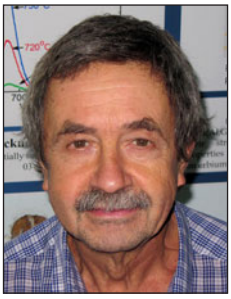


https://doi.org/10.1557/mrs.2017.29 Published online by Cambridge University Press

41. A.M. Malyarevich, I.A. Denisov, Y.V. Volk, K.V. Yumashev, O.S. Dymshits, A.A. Zhilin, *J. Alloys Compd.* **341**, 247 (2002).
42. Y.V. Volk, A.M. Malyarevich, K.V. Yumashev, O.S. Dymshits, A.V. Shashkin, A.A. Zhilin, *J. Appl. Spectrosc.* **74**, 140 (2007).
43. C. Yu, L. Chen, S. Feng, D. He, M. Wang, L. Hu, *J. Wuhan Univ. Technol.* **27**, 54 (2012).
44. P.A. Loiko, O.S. Dymshits, V.V. Vitkin, N.A. Skoptsov, A.A. Zhilin, D.V. Shemchuk, M.Y. Tsenter, K.V. Bogdanov, A.M. Malyarevich, I.V. Glazunov, X. Mateos, K.V. Yumashev, *Appl. Opt.* **55**, 5505 (2016).
45. O. Dymshits, A. Zhilin, I. Alekseeva, N. Skoptsov, A. Malyarevich, K. Yumashev, *J. Opt. Technol.* **79**, 415 (2012).
46. O. Dymshits, A. Zhilin, I. Alekseeva, N. Skoptsov, A. Malyarevich, K. Yumashev, *J. Opt. Technol.* **79**, 424 (2012).
47. O.S. Dymshits, P.A. Loiko, N.A. Skoptsov, A.M. Malyarevich, K.V. Yumashev, A.A. Zhilin, I.P. Alekseeva, M.Y. Tsenter, K. Bogdanov, *J. Non Cryst. Solids* **409**, 54 (2015).
48. O.S. Dymshits, I.P. Alekseeva, A.A. Zhilin, M.Y. Tsenter, P.A. Loiko, N.A. Skoptsov, A.M. Malyarevich, K.V. Yumashev, X. Mateos, A.V. Baranov, *J. Lumin.* **160**, 337 (2015).
49. P.A. Loiko, O.S. Dymshits, I.P. Alekseeva, A.A. Zhilin, M.Y. Tsenter, E.V. Vilejshikova, K.V. Bogdanov, X. Mateos, K.V. Yumashev, *J. Lumin.* **179**, 64 (2016). □



**Olga Dymshits** is a deputy head of the Glass Department and head of the Laboratory of Glass-Ceramics at NITIOM Vavilov State Optical Institute, Russia. She received her doctoral degree in chemistry in 1991 from the Institute of Silicate Chemistry, Russian Academy of Sciences, Russia. Her research interests include synthesis, characterization, and investigation of structure and optical properties of amorphous and nanocrystalline materials. She has published more than 100 scientific papers and holds many patents. Dymshits can be reached by phone at +7 921 864 02 17 and +7 812 560 19 11 or by email at vodym1959@gmail.com.



**Michail Shepilov** is a senior researcher in the Laboratory of Glass-Ceramics at NITIOM Vavilov State Optical Institute, Russia. He received his doctoral degree in physics from the Institute of Physics, Ukrainian Academy of Sciences, Ukraine, in 1976. He has conducted calculations of electronic band structure of fluoride and modeling of phase-transformation kinetics. His research focuses on the relationship between microstructure and light-scattering properties of glass-ceramics. He has published more than 50 scientific papers. Shepilov can be reached by phone at +7 911 9330339 or by email at m.shep@mail.ru.



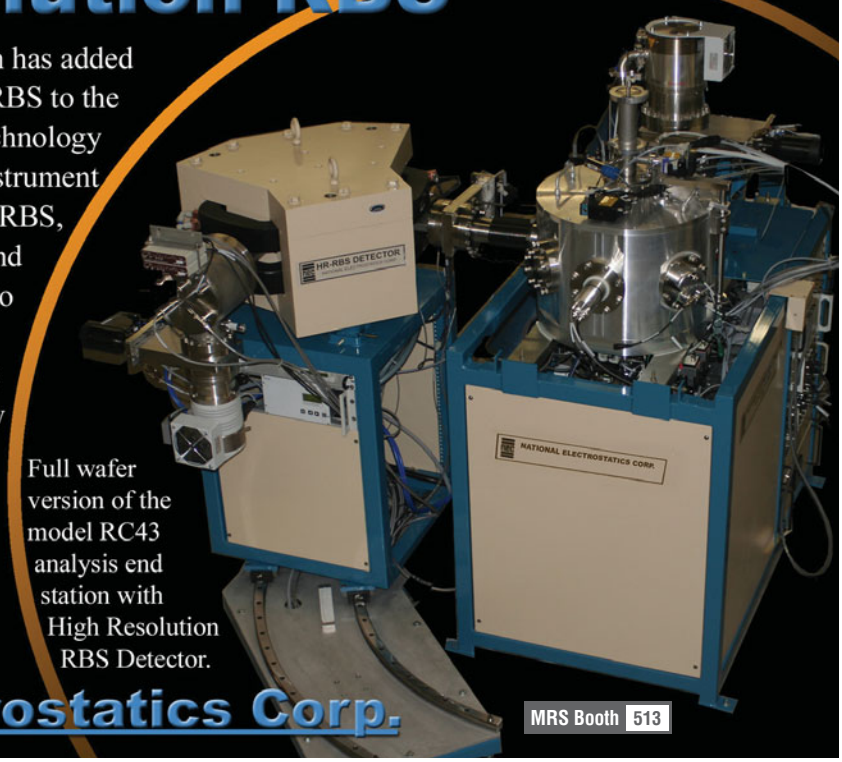
**Aleksander Zhilin** is deputy director of NITIOM Vavilov State Optical Institute, Russia. He received his doctoral degree in physical chemistry from Vavilov State Optical Institute in 1975. He has conducted investigations in areas of structure and properties of glasses and glass-ceramics. His research focuses on the optical applications of glass-ceramics. He is a member of the editorial boards of the journals *Glass Physics and Chemistry* and *Optical Technology*. He has published more than 130 scientific papers. Zhilin can be reached by phone at +7 921 9654763 or by email at zhilin1311@mail.ru.

High Resolution RBS

National Electrostatics Corporation has added Ångstrom level, High Resolution RBS to the RC43 Analysis System for nanotechnology applications. A single Pelletron instrument can now provide RBS, channeling RBS, microRBS, PIXE, ERDA, NRA, and HR-RBS capability, collecting up to four spectra simultaneously. Pelletron accelerators are available with ion beam energies from below 1 MeV in to the 100 MeV region.

www.pelletron.com
Phone: 608-831-7600
E-mail: nec@pelletron.com

Full wafer version of the model RC43 analysis end station with High Resolution RBS Detector.




National Electrostatics Corp.

MRS Booth 513



https://doi.org/10.1557/mrs.2017.29 Published online by Cambridge University Press